Simulation Model of Wind Turbine 3p Torque Oscillations due to Wind Shear and Tower Shadow

Dale S. L. Dolan, *Student Member, IEEE*, and Peter W. Lehn, *Senior Member, IEEE*

***Abstract*—To determine the control structures and possible power quality issues, the dynamic torque generated by the blades of a wind turbine must be represented. This paper presents an analytical formulation of the generated aerodynamic torque of a three-bladed wind turbine including the effects of wind shear and tower shadow. The comprehensive model includes turbine-specific parameters such as radius, height, and tower dimensions, as well as the site-specific parameter, the wind shear exponent. The model proves the existence of a 3p pulsation due to wind shear and explains why it cannot be easily identified in field measurements. The proportionality constant between the torque and the wind speed is determined allowing direct aerodynamic torque calculation from an equivalent wind speed. It is shown that the tower shadow effect is more dominant than the wind shear effect in determining the dynamic torque, although there is a small dc reduction in the torque oscillation due to wind shear. The model is suitable for real-time wind turbine simulation or other time domain simulation of wind turbines in power systems.**

***Index Terms*—Real-time digital simulation, simulation model, torque oscillations, tower shadow, wind shear, wind turbine.**

I. Introduction

TORQUE and power generated by a wind turbine is much more variable than that produced by more conventional generators. The sources of these power fluctuations are due both to stochastic processes that determine the wind speeds at different times and heights, and to periodic processes. These periodic processes are largely due to two effects termed wind shear and tower shadow. The term wind shear is used to describe the variation of wind speed with height while the term tower shadow describes the redirection of wind due to the tower structure. In three-bladed turbines, the most common [1] and largest [2] periodic power pulsations occur at what is known as a 3p frequency. This is three times the rotor frequency, or the same frequency at which the blades pass by the tower. Thus, even for a constant wind speed at a particular height, a turbine blade would encounter variable wind as it rotates. Torque pulsations and, therefore power pulsations, are observed due to the periodic variations of wind speed experienced at different locations.

Torque oscillations have been noted in several studies. It has been stated that maximum torque and power were noted when any individual blade was positioned directly downwards [3], although Thiringer [1] was unable to certify the dependence of the oscillation on wind shear. It is believed that tower shadow is also a source of the 3p oscillations observed in wind turbines although studies [1], [2] are unable to confirm this.

The 3p oscillations are important to model since they could have wide ranging effects on control systems and power quality. In systems connected directly to the grid, these torque oscillations would be important to model in terms of grid power quality. For systems interfaced to the grid through converters, these torque oscillations would be more important in terms of converter control. The torque oscillation model would be useful in studying these effects via a wind turbine simulator or other dynamic wind turbine modeling tools. Dynamic wind turbine models are needed to interface with current power system simulation tools like EMTP or PSCAD/EMTDC [4]. Existing models use either a simple aerodynamic torque representation, or are excessively complicated and not viable for incorporation into EMTP-type simulation tools [5].

Several turbine simulators have been created to model the wind turbine shaft in laboratory studies. Some simulators are capable of dynamic simulations [6]–[8] while others are only capable of performing steady-state simulations [9]. The simulator may only emulate the elements incorporated into the model. The simplest and most common approach is to use a basic steady-state torque equation to calculate wind power and use this to determine the acceleration on the turbine inertia [9]–[11]. Many of the lab simulators reviewed [8]–[13] did not include the effects of wind shear or tower shadow, making these simulators unsuitable for studying issues that may arise due to these effects.

In recent literature, dynamic models of wind turbines have been used where aerodynamic torque was either represented by steady-state torque curves [14], [15] or by simple sinusoidal oscillations [16]. This paper develops a more complete model of the wind turbine. The formulation involves a torque model for the three-bladed turbine that includes the effects of wind shear, and tower shadow. A pragmatic model appropriate for dynamic wind turbine modeling tools is not available elsewhere that incorporates these effects. The formulation will combine and build upon previous work to develop such a model. Suitable models for wind shear and tower shadow will be presented that will be put into a form from which a total wind field over the entire rotor area may be determined. A method [17] for converting a wind field into one equivalent wind speed will then be briefly reviewed. An equivalent wind speed including contributions from the hub height wind speed, wind shear and tower shadow will be calculated. Finally, a completed normalized torque model will be presented that is suitable for implementation in a real-time wind turbine simulator or other time domain simulation.

Manuscript received March 31, 2005. Paper no. TEC-00137-2005.

The authors are with the Department of Electrical and Computer Engineering, University of Toronto, Toronto, ON M5S 3G4, Canada (e-mail: dale.dolan@utoronto.ca; lehn@ecf.utoronto.ca).

Digital Object Identifier 10.1109/TEC.2006.874211

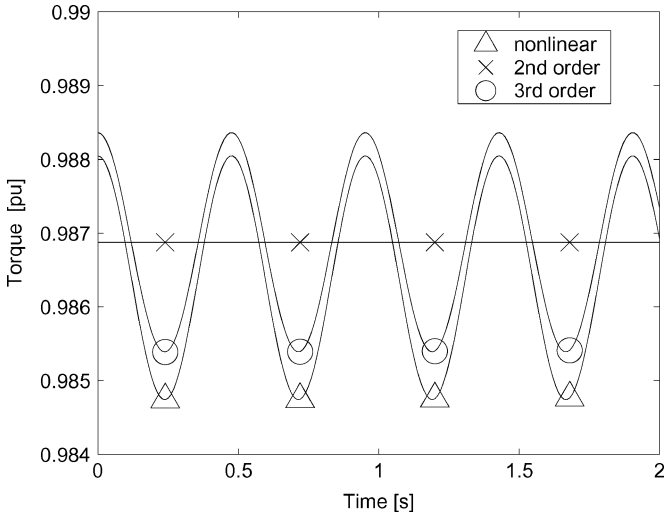

Fig. 1. Comparison of torque oscillation due to wind shear alone depending on form of wind shear approximation.

II. Wind Shear

Wind speed generally increases with height and this variation is termed wind shear. Torque pulsations, and therefore power pulsations, are observed due to the periodic variations of wind speed seen at different heights. Power and torque oscillate due to the different wind conditions encountered by each blade as it rotates through a complete cycle [3]. For instance, a blade pointing upwards would encounter wind speeds greater than a blade pointing downwards. During each rotation, the torque oscillates three times because of each blade passing through minimum and maximum wind.

It is therefore important to model these wind-shear-induced 3p torque pulsations when studying a wind turbine system. A common wind shear model, shown as (1), is taken directly from the literature on wind turbine dynamics [1], [18], [19].

$$V(z) = V_{\mathrm{H}} \left(\frac{z}{H}\right)^{\alpha} \tag{1}$$

For the purpose of this analysis, (1) is converted to a function of r (radial distance from rotor axis) and θ (azimuthal angle) giving the following:

$$V(r,\theta) = V_{\mathrm{H}} \left(\frac{r\cos\theta + H}{H}\right)^{\alpha} = V_{\mathrm{H}}[1 + W_{\mathrm{s}}(r,\theta)] \tag{2}$$

where V_{H} is the wind speed at hub height, r is the radial distance from rotor axis, W_{s} is the wind-shear-shape function [18], α is the empirical wind shear exponent, H is the elevation of rotor hub, and z is the elevation above ground. The term $W_{\mathrm{s}}(r,\theta)$ is the disturbance seen in wind speed due to wind shear that is added to hub height wind speed.

Both Spera [18] and Thresher [19] approximated $W_s(r,\theta)$ by the second-order-truncated Taylor series expansion shown as follows:

$$W_s(r,\theta) \approx \alpha \left(\frac{r}{H}\right)\cos\theta + \frac{\alpha(\alpha-1)}{2}\left(\frac{r}{H}\right)^2 \cos^2\theta \tag{3}$$

However, as shown in Fig. 1, the truncated expansion of (3) eliminates, in three-bladed turbines, the torque oscillations due to the wind shear when the contributions from each of the blades are summed. This is because when the three blade contributions are summed, the $\cos\theta$ term yields a zero contribution while the $\cos^2\theta$ term contributes only a dc component that adjusts average wind speed from hub height wind speed to spatial mean wind speed. This can be seen in Fig. 1, where the resulting torque from the second order approximation becomes constant, completely losing the properties of the nonlinear wind shear expression. To effectively model the 3p effect of wind shear, a $\cos^3\theta$ term is necessary, requiring a third-order-truncated Taylor expansion. Therefore, to model torque oscillations from wind shear, the approximation used for $W_s(r,\theta)$ should be as follows.

$$W_s(r,\theta) \approx \alpha \left(\frac{r}{H}\right)\cos\theta + \frac{\alpha(\alpha-1)}{2}\left(\frac{r}{H}\right)^2 \cos^2\theta + \frac{\alpha(\alpha-1)(\alpha-2)}{6}\left(\frac{r}{H}\right)^3 \cos^3\theta \tag{4}$$

III. Tower Shadow

The distribution of wind is altered by the presence of the tower. For upwind rotors, the wind directly in front of the tower is redirected and thereby reduces the torque at each blade when in front of the tower. This effect is called tower shadow. The torque pulsations due to tower shadow are most significant when a turbine has blades downwind of the tower and wind is blocked as opposed to redirected [20]. For this reason, the majority of modern wind turbines have upwind rotors. This paper will therefore only deal with the tower shadow torque oscillations in horizontal axis three-bladed upwind rotors. This section will show theoretically the 3p oscillations caused by tower shadow.

The wind field, only considering tower shadow, is defined as in (5), where V_{H} = hub height wind speed. The term $v_{\mathrm{tower}}(y,x)$ is the disturbance observed in the wind speed due to the tower shadow that is added to hub height wind speed. Sorensen [17] modeled tower disturbance using potential flow theory for wind movement around the tower. Using the reference frames shown in Fig. 2 yields (6).

$$V(y,x) = V_{\mathrm{H}} + v_{\mathrm{tower}}(y,x) \tag{5}$$

$$v_{\mathrm{tower}}(y,x) = V_0 a^2 \frac{y^2 - x^2}{(x^2+y^2)^2} \tag{6}$$

In (6), V_0 is the spatial mean wind speed, a is the tower radius, y is the lateral distance from the blade to the tower midline, and x is the distance from the blade origin to the tower midline.

Results for tower radius of 2 m and four different longitudinal distances between the tower and the blades are shown in Fig. 3. It can be seen that as expected, the tower shadow effect is more pronounced when the blades are closer (x smaller) to the tower.

An alternate tower-shadow-deficit model (7) is developed in [21] and shown as follows:

$$v_{\mathrm{tower}}(y,x) = -V_0 \frac{D}{2\pi}\frac{x}{(x^2+y^2)} \tag{7}$$

where D is the tower diameter, y is the lateral distance from the blade to the tower midline, x is the distance from the blade

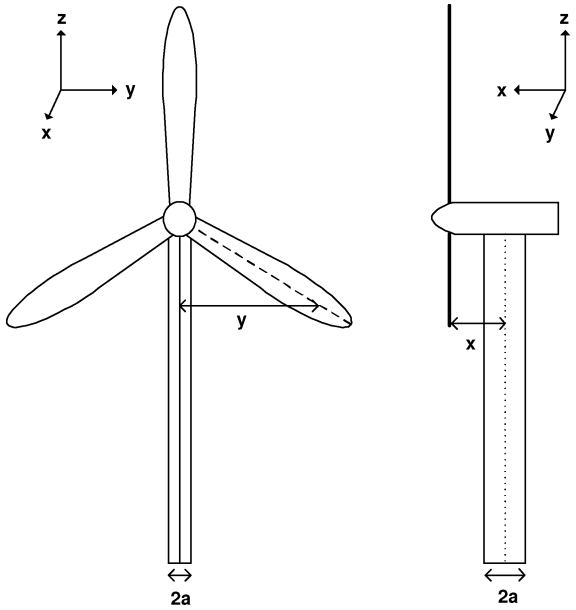

Fig. 2. Dimensions used in tower shadow formula.

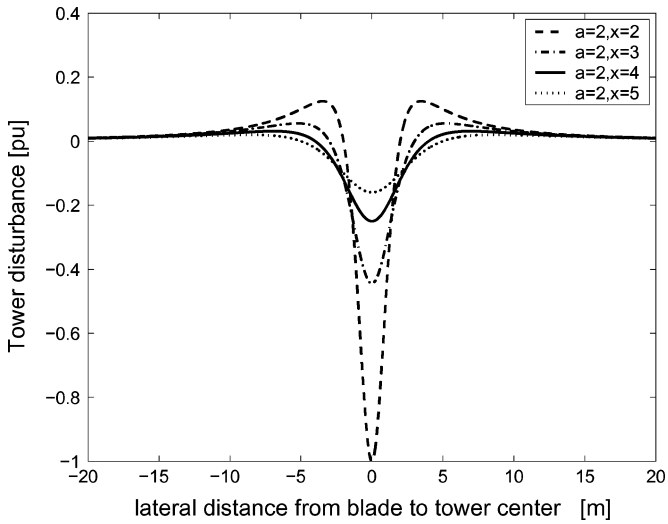

Fig. 3. Comparison of tower shadow model (6) with different distances between the tower and the blades.

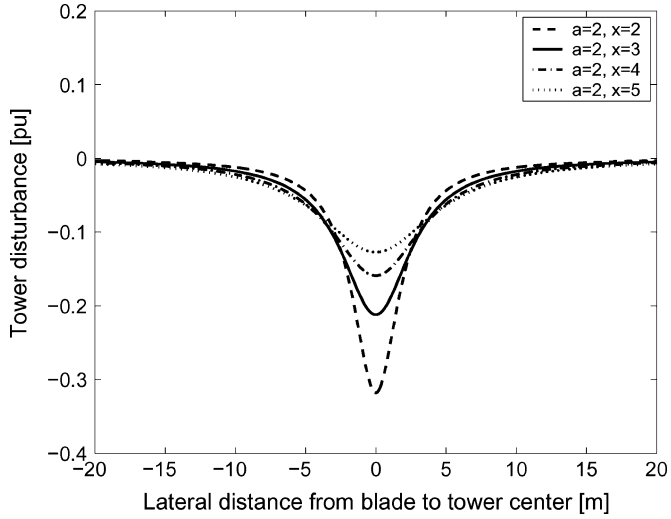

Fig. 4. Comparison of tower shadow model (7) with different distances between the tower and the blades.

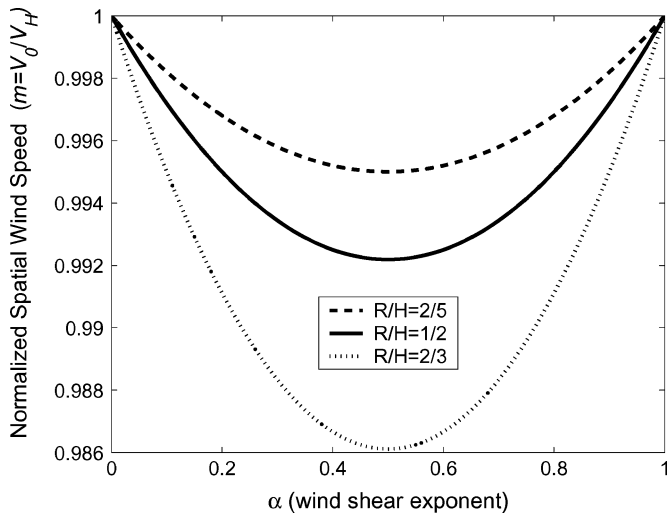

Fig. 5. Variation of $m = V_0/V_{\rm H}$ with α for different R/H ratios.

origin to the tower midline, and V_0 is the spatial mean wind speed. Results for this alternate model with a tower radius of 2 m and four different longitudinal distances between the tower and the blades are shown in Fig. 4.

Comparison of the two models graphically shows that a more reasonable model is represented by (6), as it models both the deceleration of the wind flow in front of the tower and the acceleration of the wind flow on each side of the tower. Therefore, for modeling torque oscillations due to tower shadow, (6) is preferable and will be used in subsequent model development.

Different reference wind speeds are used in models for the disturbance due to wind shear and tower shadow. The wind shear model uses hub height wind speed $(V_{\rm H})$ while the tower shadow model uses spatial mean wind speed (V_0). The relationship between these two wind speeds is formulated in Appendix and is summarized in Fig. 5. Most often for time-domain simulation, only a single wind speed value, $V_{\rm H}$, is available. V_0 would require calculation from an entire spatial wind field that would normally be unavailable. Therefore, for all practical purposes, in the torque oscillation model, tower disturbance will be expressed in terms of $V_{\rm H}$. Converting (6) from a function of y (lateral distance) to a function of r (radial distance) and θ (azimuthal angle) normalized to $V_{\rm H}$ yields as follows:

$$\tilde{v}_{\rm tower}(r,\theta,x) = ma^2 \frac{r^2\sin^2(\theta) - x^2}{(r^2\sin^2(\theta)+x^2)^2} \tag{8}$$

where a is the tower radius, r is the radial distance from the blade to the hub center, θ is the azimuthal angle of the blade, x is the distance from the blade origin to the tower midline, and $m = [1 + \frac{\alpha(\alpha-1)(R^2)}{8H^2}]$ as developed in Appendix. It should be noted that (8) is only valid for $90^\circ \le \theta \le 270^\circ$ as above the horizontal, tower shadow effects should obviously be absent.

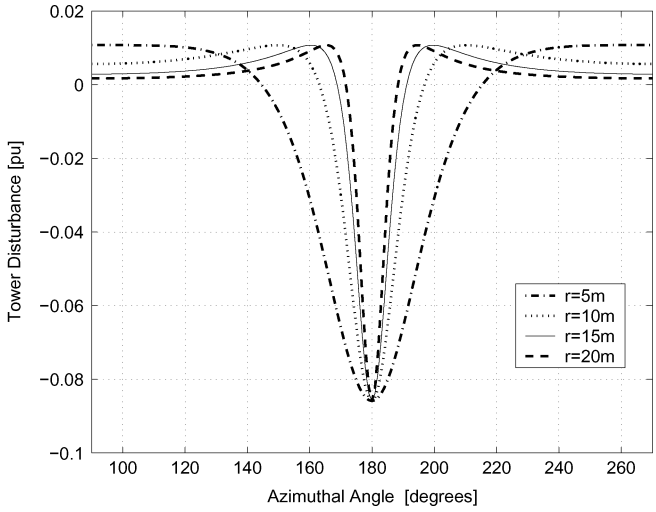

Fig. 6. Comparison of tower shadow at different radii based on a tower with 1.7-m diameter and blades 2.9 m from tower midline.

Fig. 6 shows the variation in the effective tower shadow angle experienced by different blade elements at varying radial distances. It is observed that the blade elements closer to the hub experience tower shadow for a longer period, although the same wind deficit is seen for all blade elements at an angle of 180°.

IV. Determination of Total Wind Field—$v(t, r, \theta)$

To determine the total wind field, the results of (4) and (8) from Sections II and III are combined. The total wind field due to both tower shadow and wind shear is given as follows.

$$v(t,r,\theta) = V_{\rm H}(t)[1 + W_s(r,\theta)][1 + \tilde{v}_{\rm tower}(r,\theta,x)] \quad (9)$$

$$v(t,r,\theta) = V_{\rm H}(t)[1 + W_s(r,\theta) + \tilde{v}_{\rm tower}(r,\theta,x) + W_s(r,\theta)\tilde{v}_{\rm tower}(r,\theta,x)]. \quad (10)$$

As $W_s(r,\theta)\tilde{v}_{\rm tower}(r,\theta,x)$ would be small compared to other terms, (11) is a valid approximation of (9). This approach is also supported in the literature [19].

$$v(t,r,\theta) \approx V_{\rm H}(t)[1 + W_s(r,\theta) + \tilde{v}_{\rm tower}(r,\theta,x)] \quad (11)$$

The spatially varying wind speed can be calculated using the total wind field model of (11) or its expanded version as follows.

$$v(t,r,\theta) \approx V_{\rm H}(t)\Bigg[1 + \alpha\left(\frac{r}{H}\right)\cos\theta + \frac{\alpha(\alpha-1)}{2}\left(\frac{r}{H}\right)^2\cos^2\theta + \frac{\alpha(\alpha-1)(\alpha-2)}{6}\left(\frac{r}{H}\right)^3\cos^3\theta + \frac{ma^2(r^2\sin^2\theta - x^2)}{(r^2\sin^2\theta + x^2)^2}\Bigg]. \quad (12)$$

This total wind field model allows one to determine the wind speed observed at any particular location in the rotor disk area, knowing only the turbine parameters, wind shear coefficient and a single hub height wind speed.

V. Equivalent Wind Speed Formulation Based on Equivalent Torque

An effective method for formulating an "equivalent wind speed" has been developed by Sorensen [17]. The equivalent wind speed is a representation of the actual spatially varying wind speed that is defined such that it will give the same aerodynamic torque. The advantage of this method is that a wind speed without radial dependence may be used. For clarity and completeness, Sorensen's approach is briefly outlined in this section.

The aerodynamic torque produced by a three-bladed wind turbine immersed in a wind field $v(t,r,\theta)$ is given as follows:

$$T_{\rm ae}(t,\theta) = 3M(V_0) + \sum_{b=1}^{3}\int_{r_0}^{R}\psi(r)[v(t,r,\theta_b) - V_0]\,dr \quad (13)$$

where $T_{\rm ae}(t,\theta)$ is the aerodynamic torque, $M(V_0)$ is the steady-state blade root moment resulting from spatial mean wind speed V_0, R is the radius of the rotor disk, r_0 is the radius at which blade profile begins, and $\psi(r)$ is the influence coefficient of the aerodynamic load on the blade root moment. This equation has been determined through linearization of individual blade torque dependence on wind speed [17].

An equivalent wind speed $v_{\rm eq}(t,\theta)$ that does not vary with the radius is defined which would give the same aerodynamic torque as the actual spatially varying wind speed. This $v_{\rm eq}$ must be such that

$$T_{\rm ae}(t,\theta) = 3M(V_0) + \sum_{b=1}^{3}\int_{r_0}^{R}\psi(r)[v_{\rm eq}(t,\theta) - V_0]\,dr. \quad (14)$$

Sorensen determined (15) to be the expression for equivalent wind speed by equating (13) and (14)

$$v_{\rm eq}(t,\theta) = \frac{1}{3}\sum_{b=1}^{3}\frac{\int_{r_0}^{R}\psi(r)v(t,r,\theta_b)dr}{\int_{r_0}^{R}\psi(r)\,dr} \quad (15)$$

VI. Determination of Equivalent Wind Speed

The total wind field including tower shadow and wind shear effects will now be converted into one equivalent wind speed. Three components of this equivalent wind speed will be separated and solved individually such that the effects from the hub height wind speed, wind shear, and tower shadow may be observed separately.

Assuming $\psi(r) = kr$, and defining $n = \frac{r_0}{R}$ and $s = 1 - n^2$, the total wind field (11) may be inserted into (15) to yield (16) after some initial simplification.

$$v_{\rm eq}(t,\theta) = \frac{2V_{\rm H}}{3sR^2}\sum_{b=1}^{3}\int_{r_0}^{R}\Bigg[r + \frac{r^2\alpha}{H}\cos\theta_b + \frac{r^3\alpha(\alpha-1)}{2H^2}\cos^2\theta_b + \frac{r^4\alpha(\alpha-1)(\alpha-2)}{6H^3}\cos^3\theta_b + \frac{ma^2(r^3\sin^2\theta_b - rx^2)}{(r^2\sin^2\theta_b + x^2)^2}\Bigg]dr. \quad (16)$$

This equivalent wind speed will have three components. The first $(v_{\rm eq_0})$ is due to the hub height wind speed, the second $(v_{\rm eq_{ws}})$ is due to the wind shear, and the third $(v_{\rm eq_{ts}})$ is due to

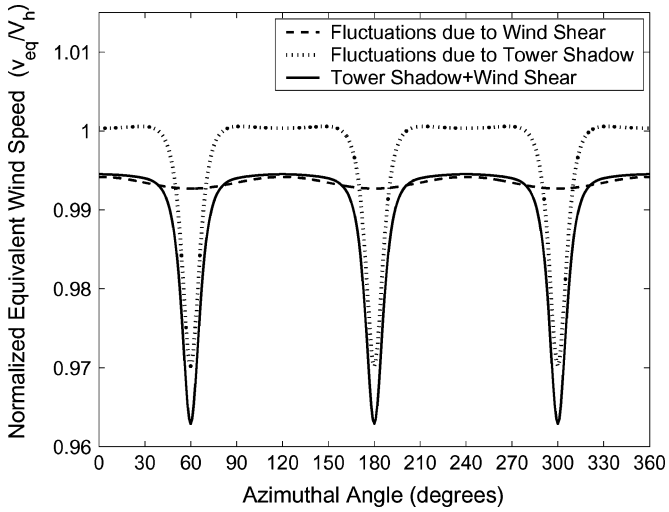

Fig. 7. Normalized equivalent wind speed due to tower shadow ($v_{\mathrm{eq_{ts}}} + v_{\mathrm{eq_0}}$), wind shear ($v_{\mathrm{eq_{ws}}} + v_{\mathrm{eq_0}}$), and combination of wind shear and tower shadow ($v_{\mathrm{eq_0}} + v_{\mathrm{eq_{ts}}} + v_{\mathrm{eq_{ws}}}$).

the tower shadow. Therefore, (16) can be decomposed as (17) whose components are shown as (18)–(20).

$$v_{\mathrm{eq}}(t,\theta) = v_{\mathrm{eq_0}} + v_{\mathrm{eq_{ws}}} + v_{\mathrm{eq_{ts}}} \tag{17}$$

$$v_{\mathrm{eq_0}} = \frac{2V_{\mathrm{H}}}{3sR^2}\sum_{b=1}^{3}\int_{r_0}^{R}[r]\,dr \tag{18}$$

$$v_{\mathrm{eq_{ws}}} = \frac{2V_{\mathrm{H}}}{3sR^2}\sum_{b=1}^{3}\int_{r_0}^{R}\left[\frac{r^2\alpha}{H}\cos\theta_b + \frac{r^3\alpha(\alpha-1)}{2H^2}\cos^2\theta_b + \frac{r^4\alpha(\alpha-1)(\alpha-2)}{6H^3}\cos^3\theta_b\right]dr \tag{19}$$

$$v_{\mathrm{eq_{ts}}} = \frac{2V_{\mathrm{H}}}{3sR^2}\sum_{b=1}^{3}\int_{r_0}^{R}\left[\frac{ma^2(r^3\sin^2\theta_b - rx^2)}{(r^2\sin^2\theta_b + x^2)^2}\right]dr. \tag{20}$$

Using the results derived in this section, the normalized equivalent wind speeds were determined for a turbine with the following representative specifications: $R = 20, H = 40$, $\alpha = 0.3, a = 0.85$, and $x = 2.9$. The normalized equivalent wind speed, caused by the tower shadow and the wind shear both together and individually, of this configuration are shown in Fig. 7. It is seen that the effect of the tower shadow is more dominant than the effect of the wind shear.

A. Solving for $v_{\mathrm{eq_0}}$

This brief section will calculate the component of the equivalent wind speed that is due to the steady-state hub height wind speed. As expected and shown by (22), this component is simply equal to the hub height wind speed, V_{H}. It can be seen that this result is independent of the values of r_0, n, and s.

$$v_{\mathrm{eq_0}} = \frac{2V_{\mathrm{H}}}{3sR^2}\sum_{b=1}^{3}\left[\frac{sR^2}{2}\right]dr \tag{21}$$

$$v_{\mathrm{eq_0}} = V_{\mathrm{H}}. \tag{22}$$

B. Solving for $v_{\mathrm{eq_{ws}}}$

The component of the equivalent wind speed that is due to the wind shear is calculated in this section and is given as (28). Through numerical analysis, it was found that for a conservative estimate of $r_0 = 0.1R$, that $v_{\mathrm{eq_{ws}}}$ was comparable to the case where $r_0 = 0$. Therefore, for the development, r_0 will be taken as equal to 0 to simplify equations allowing $n = 0$ and $s = 1$. If desired, a true value of r_0 may be used without much more computational effort.

$$v_{\mathrm{eq_{ws}}} = \frac{2V_{\mathrm{H}}}{3R^2}\sum_{b=1}^{3}\left[\frac{R^3}{3}\frac{\alpha}{H}\cos\theta_b + \frac{R^4}{4}\frac{\alpha(\alpha-1)}{2H^2}\cos^2\theta_b + \frac{R^5}{5}\frac{\alpha(\alpha-1)(\alpha-2)}{6H^3}\cos^3\theta_b\right]. \tag{23}$$

To further simplify (23), expressions for the sums must be developed. Using trigonometric identities and the angle definitions shown in (24), these sums are determined and shown in the form of (25)–(27) as follows.

$$\theta = \theta_1, \theta_2 = \theta_1 + \frac{2\pi}{3} \quad \text{and} \quad \theta_3 = \theta_1 + \frac{4\pi}{3} \tag{24}$$

$$\sum_{b=1}^{3}[\cos\theta_b] = 0 \tag{25}$$

$$\sum_{b=1}^{3}[\cos^2\theta_b] = \frac{3}{2} \tag{26}$$

$$\sum_{b=1}^{3}[\cos^3\theta_b] = \frac{3}{4}\cos 3\theta. \tag{27}$$

We can now substitute (25)–(27) into (23) to yield the final expression for equivalent wind speed due to wind shear as follows:

$$v_{\mathrm{eq_{ws}}} = V_{\mathrm{H}}\left[\frac{\alpha(\alpha-1)}{8}\left(\frac{R}{H}\right)^2 + \frac{\alpha(\alpha-1)(\alpha-2)}{60}\left(\frac{R}{H}\right)^3\cos 3\theta\right]. \tag{28}$$

The normalized equivalent wind speed caused by the wind shear added to equivalent wind speed due to hub height wind speed ($v_{\mathrm{eq_{ws}}} + v_{\mathrm{eq_0}}$) is shown in Fig. 7. It can be observed that this has a minimum when one blade is pointed directly downwards but is a relatively small effect ($\ll 1\%$). It is also seen that there is a reduction in the equivalent wind speed due to wind shear when normalized to V_{H}. In this case this depression is $\approx 0.5\%$.

C. Solving for $v_{\mathrm{eq_{ts}}}$

The component of the equivalent wind speed that is due to the tower shadow is calculated and is given in its final form as (30). The formulation begins by performing the integration

within (20) to yield (29).

$$v_{\mathrm{eq_{ts}}} = \frac{2mV_{\mathrm{H}}}{3sR^2}\sum_{b=1}^{3}\left[\frac{a^2\ln\left(R^2\sin^2\theta_b + x^2\right)}{2\sin^2\theta_b} - \frac{a^2\ln\left(r_0^2\sin^2\theta_b + x^2\right)}{2\sin^2\theta_b} + \frac{a^2x^2}{\sin^2\theta_b\left(R^2\sin^2\theta_b + x^2\right)} - \frac{a^2x^2}{\sin^2\theta_b\left(r_0^2\sin^2\theta_b + x^2\right)}\right]. \tag{29}$$

Numerical evaluation shows that (29) gives nearly identical results with $r_0 = 0.1R$ and $r_0 = 0$. Therefore, to further simplify (29), it will be assumed that $r_0 = 0$ and therefore $s = 1$. This allows for the simplification of (29) to (30).

$$v_{\mathrm{eq_{ts}}} = \frac{mV_{\mathrm{H}}}{3R^2}\sum_{b=1}^{3}\left[\frac{a^2}{\sin^2\theta_b}\ln\left(\frac{R^2\sin^2\theta_b}{x^2} + 1\right) - \frac{2a^2R^2}{R^2\sin^2\theta_b + x^2}\right]. \tag{30}$$

The normalized equivalent wind speed caused by the tower shadow added to the equivalent wind speed due to the hub height wind speed ($v_{\mathrm{eq_{ts}}} + v_{\mathrm{eq_0}}$) is shown in Fig. 7. It can be seen that this has a minimum when a blade is directly downwards and at $\approx$3%, is much larger than the effect from the wind shear.

VII. Extraction of Function $\psi(r)$

A typical distribution of aerodynamic load can assume that $\psi(r)$ is proportional to r [17]. However, to use the equivalent wind speed to calculate torque oscillations the proportionality constant must be known. This value is not specified in the literature and thus must be determined. To extract the proportionality constant we must linearize the classic torque equation's (31) dependence on wind speed. Since (13) is itself derived through linearization, this may be done without additional loss of generality. We use an operating point around V_0, since the steady-state torque depends on the spatial mean wind speed.

$$T_{\mathrm{ae}}(t,\theta) = \frac{1}{2}\rho AV^2R\frac{C_p(\lambda)}{\lambda}. \tag{31}$$

Linearizing (31), we get (32), where V_0 is the spatial mean wind speed and λ_0 is the tip speed ratio at V_0.

$$T_{\mathrm{ae}}(t,\theta) = T_{\mathrm{ae}}(t,\theta)\left|_{\substack{V=V_0\\ \lambda=\lambda_0}} + \frac{\partial T_{\mathrm{ae}}(t,\theta)}{\partial V}\right|_{\substack{V=V_0\\ \lambda=\lambda_0}}\Delta V = \frac{1}{2}\rho A{V_0}^2R\frac{C_p(\lambda_0)}{\lambda_0} + \rho AV_0R\frac{C_p(\lambda_0)}{\lambda_0}\Delta V. \tag{32}$$

Defining $n = \frac{r_0}{R}$ and $s = 1 - n^2$, and with $\Delta V = v_{\mathrm{eq}}(t,\theta) - V_0$, (14) may now be transformed to (34).

$$T_{\mathrm{ae}}(t,\theta) = 3M(V_0) + \sum_{b=1}^{3}\int_{r_0}^{R} kr\Delta V\,dr \tag{33}$$

$$T_{\mathrm{ae}}(t) = 3M(V_0) + 3k\frac{sR^2}{2}\Delta V. \tag{34}$$

Equating (32) and (34) yields two new important results, shown as follows.

$$3M(V_0) = \frac{1}{2}\rho AV_0^2R\frac{C_p(\lambda_0)}{\lambda_0} \tag{35}$$

$$k = \frac{2\rho AV_0}{3sR}\frac{C_p(\lambda_0)}{\lambda_0}. \tag{36}$$

The first result (35) shows that the addition of the steady-state blade root moments over the three blades $[3M(V_0)]$ is equivalent to the classic torque equation (31) at a particular wind speed. The second result (36) gives the proportionality constant between the torque deviation from the steady-state torque and the wind speed deviation from the average wind speed. This new result is important since it allows direct calculation of aerodynamic torque from equivalent wind speed.

VIII. Torque Oscillations

With the three formulations of equivalent wind speed components, the overall torque oscillations can now be modeled. Using the linearized aerodynamic torque relation (34) and allowing $\Delta V = v_{\mathrm{eq}}(t,\theta) - V_0$ and $V_0 = mV_{\mathrm{H}}$, we get the following results:

$$T_{\mathrm{ae}}(t,\theta) = 3M(V_0) + \frac{3ksR^2}{2}[v_{\mathrm{eq}}(t,\theta) - V_0] \tag{37}$$

$$T_{\mathrm{ae}}(t,\theta) = 3M(V_0) + \frac{3ksR^2}{2} \times [v_{\mathrm{eq_{ws}}} + v_{\mathrm{eq_{ts}}} + V_{\mathrm{H}} - mV_{\mathrm{H}}]. \tag{38}$$

Normalizing (38) to torque at wind speed V_0, we get the expression

$$\overline{T_{\mathrm{ae}}(t,\theta)} = 1 + \frac{2}{mV_{\mathrm{H}}}[v_{\mathrm{eq_{ws}}} + v_{\mathrm{eq_{ts}}} + (1-m)V_{\mathrm{H}}]. \tag{39}$$

Using the end result of the formulation (39), the torque oscillations were determined for a turbine with the following representative specifications: $R = 20, H = 40, \alpha = 0.3, a = 0.85$, and $x = 2.9$. As an illustration of possible results of the modeling, the normalized torque oscillations due to wind shear and tower shadow alone, as well as the total torque oscillations of this configuration are shown in Fig. 8. Again it is observed that the effects of wind shear on the total aerodynamic torque are much smaller than those due to tower shadow, although they do reshape the curve in regions. It is observed that both the oscillations due to wind shear and tower shadow have a minimum when one blade is pointed directly downwards and a maximum when one blade is pointing directly upwards. The wind shear effect is relatively small ($\ll$1%), while the effect of the tower shadow is much larger, in this case approximately 6% of the total aerodynamic torque. It is also seen that there is a small ($\approx$1%) negative dc offset in the torque oscillation due to wind shear. This offset seems to disappear in the total torque. This is due to the normalization by a steady-state torque that occurs at V_0. As this dc offset is already contained in the $3M(V_0)$ term of (38), its duplication in the wind shear term is corrected for by the $(1-m)V_{\mathrm{H}}$ term.

Dependence of the total 3p pulsation on wind shear exponent (α) and dependence of wind-shear-induced 3p pulsation on

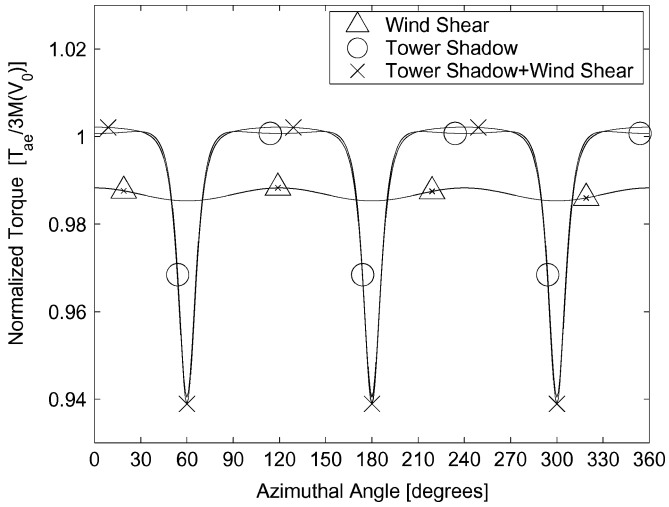

Fig. 8. Resulting normalized aerodynamic torque due to wind shear $(1 + \frac{2}{mV_{\rm H}} v_{\rm eq_{ws}})$, tower shadow $(1 + \frac{2}{mV_{\rm H}} v_{\rm eq_{ts}})$, and combination of wind shear and tower shadow $(1 + \frac{2}{mV_{\rm H}} v_{\rm eq_{ts}} + \frac{2}{mV_{\rm H}} v_{\rm eq_{ws}} + \frac{2(1-m)}{m})$.

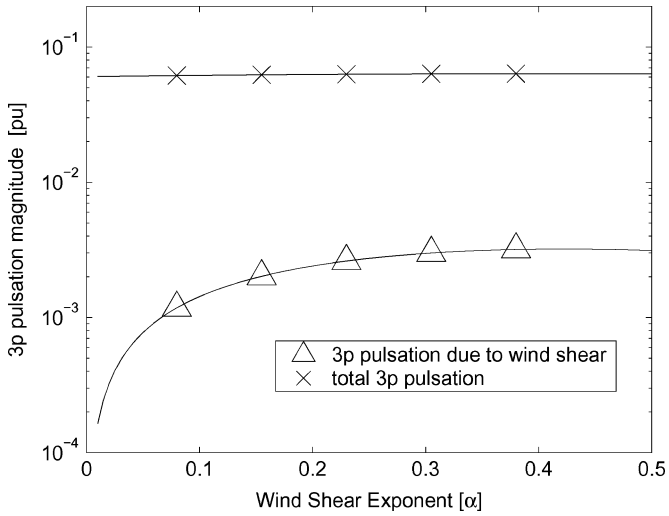

Fig. 9 Relative magnitude (per unit mean torque) of 3p pulsation as a function of wind shear exponent (α).

α is shown in Fig. 9. As observed in the graph, although a correlation is seen between α and the wind-shear-induced 3p pulsation, no significant correlation is observed between α and the total 3p pulsation.

IX. Discussion

The torque model gives two particularly interesting results. The first is that the tower shadow effects are much more dominant than are the wind shear effects. The second is that the maximum torque is observed when a blade is pointing directly upwards. The modeled torque oscillations clearly depend on turbine parameters R, H, a, and x and site parameter α. The wind shear component of the oscillations depends on R, H, and α and the tower shadow component of the oscillations depends mainly on R, a, and x.

The wind shear exponent obviously has an effect on the torque oscillations due to wind shear. However, as seen in Fig. 9, there is not a significant correlation between α and the total 3p pulsation. This is due to the wind-shear-induced component being approximately only 5% of the tower-shadow-induced component. This explains why Thiringer was unable to find a good correlation between α and measured 3p pulsation [1].

In Fig. 9, maximal oscillations occur at a value of $\alpha = 0.423$, where the oscillations are approximately 50% larger than those observed for a typical value of α, such as that used to generate Fig. 8. As seen in the figure, this would still result in a very small oscillation. For wind shear, the actual magnitude of R and H are not critical as it is only their ratio that has an effect. Typically, $\frac{2}{5} \leq \frac{R}{H} \leq \frac{2}{3}$. The higher the ratio, the greater the effect the wind shear would have as there is a wider range of wind speeds that the blade experiences in a rotation. For a ratio of $\frac{2}{3}$, the torque oscillation is five times larger than that observed for a ratio of $\frac{2}{5}$. However, combining the effects of these two parameters to yield maximal torque oscillations still only amounts to a peak value of approximately 0.4% of steady-state torque. Although this torque oscillation is a relatively small one compared to the tower-shadow-induced oscillations, it is still included in the pragmatic model. This is done for three reasons. First, the effect is quite easy to include as it can be represented in a closed form expression. Second the model also contributes a dc component that modifies the average torque, and lastly the torque oscillation reshapes the curve at the peak torque.

For tower shadow, the actual radius of the turbine, independent of height, is important. A larger turbine radius results in both a narrower angle where a torque reduction is seen as well as a slightly smaller reduction in overall torque. As can be easily observed by the formula for equivalent wind speed due to the tower shadow (30), the radius of the tower has a squared relationship with total torque disturbance. Doubling of the tower radius will give a fourfold increase in torque disturbance. The distance from the tower (x) is also an important factor. The closer the blades are to the tower, the larger the effect of the tower shadow.

X. Conclusion

A comprehensive yet pragmatic torque model has been developed for the three-bladed wind turbine. The model proves the existence of wind-shear-induced 3p oscillations and demonstrates that in practice, their presence is masked by the much larger tower-shadow-induced oscillations. It is determined that maximum torque is seen when a blade is pointing directly upwards for both wind shear and tower shadow effects. The modeled torque oscillations depend mostly on R, a, and x, as these are related to tower shadow. Although wind shear causes small 3p oscillations, it also contributes approximately a 1% dc reduction in average torque. The proportionality constant between wind speed variations and torque oscillations is determined, allowing direct aerodynamic torque calculation from an equivalent wind speed. This model is a useful representation of the aerodynamic torque of a wind turbine for use in real-time wind turbine simulators and other dynamic-model-simulation-based applications.

APPENDIX

A relationship between spatial average wind speed V_0 and hub height wind speed $V_{\rm H}$ is required such that tower shadow and wind shear formulas can be combined with only one wind speed term. To calculate spatial average wind speed V_0, the varying wind speed from wind shear is integrated over rotor area and divided by the total rotor area.

$$V_0 = \frac{1}{\pi R^2}\int_0^{2\pi}\int_0^R V_{\rm H}[1+W_s(r,\theta)]r\,dr\,d\theta \tag{40}$$

$$V_0 = \frac{1}{\pi R^2}\int_0^{2\pi}\int_0^R V_{\rm H}\left[1+\alpha(\frac{r}{H})\cos\theta + \frac{\alpha(\alpha-1)}{2}\left(\frac{r}{H}\right)^2\cos^2\theta + \frac{\alpha(\alpha-1)(\alpha-2)}{6}\left(\frac{r}{H}\right)^3\cos^3\theta\right]r\,dr\,d\theta \tag{41}$$

$$V_0 = \frac{V_{\rm H}}{\pi R^2}\int_0^R\left[2\pi r + \frac{\pi\alpha(\alpha-1)r^3}{2H^2}\right]dr \tag{42}$$

$$V_0 = \frac{V_{\rm H}}{\pi R^2}\left[2\pi\frac{R^2}{2} + \frac{\pi\alpha(\alpha-1)R^4}{8H^2}\right] \tag{43}$$

$$V_0 = V_{\rm H}\left[1+\frac{\alpha(\alpha-1)(R^2)}{8H^2}\right] = mV_{\rm H}. \tag{44}$$

In (40)–(44), $V_{\rm H}$ is the wind speed at hub height, R is the blade radius, α is the empirical wind shear exponent, and H is the elevation of rotor hub.

It is shown in Fig. 5 that $0.986 < \frac{V_0}{V_{\rm H}} \leq 1$, for $\frac{R}{H} < 0.67$ and $0.1 < \alpha \leq 1$. Therefore, for most cases a simplification that $V_0 = V_{\rm H}$ is justified. For more accuracy (44) can be used.

REFERENCES

[1] T. Thiringer and J.-A. Dahlberg, "Periodic pulsations from a three-bladed wind turbine," *IEEE Trans. Energy Convers.*, vol. 16, pp. 128–133, Jun. 2001.

[2] T. Thiringer, "Power quality measurements performed on a low-voltage grid equipped with two wind turbines," *IEEE Trans. Energy Convers.*, vol. 11, pp. 601–606, Sep. 1996.

[3] S. B. Bayne and M. G. Giesselmann, "Effect of blade passing on a wind turbine output," in *Proc. Energy Conversion Engineering Conf. Exhib., (IECEC) 35th Intersociety*, Jul. 2000, vol. 2, pp. 775–781.

[4] J. G. Slootweg, S. W. H. de Haan, H. Polinder, and W. L. Kling, "General model for representing variable speed wind turbines in power system dynamics simulations," *IEEE Trans. Power Syst.*, vol. 18, no. 1, pp. 144–151, Feb. 2003.

[5] T. Petru and T. Thiringer, "Modeling of wind turbines for power system studies," *IEEE Trans. Power Syst.*, vol. 17, no. 4, pp. 1132–1139, Nov. 2002.

[6] D. S. L. Dolan, "Real-time wind turbine emulator suitable for power quality and dynamic control studies" MASc. thesis, Dept. Electr. Comput. Eng., Univ. Toronto, Toronto, 2005.

[7] D. S. L. Dolan and P. W. Lehn, "Real-time wind turbine emulator suitable for power quality and dynamic control studies," presented at the Int. Conf. Power Systems Transients, IPST05, Montreal, Canada, Jun. 19–23 2005.

[8] R. Cardenas, R. Pena, G. M. Asher, and J. C. Clare, "Experimental emulation of wind turbines and flywheels for wind energy applications," presented at the *EPE Conf.*, Graz, Austria, Aug. 2001.

[9] L. Chang, R. Doraiswami, T. Boutot, and H. Kojabadi, "Development of a wind turbine simulator for wind energy conversion systems," in *Proc. Canadian IEEE CCECE 2000*, vol. 1, Halifax, Canada, 2000, pp. 550–554.

[10] F. A. Farret, R. Gules, and J. Marian, "Micro-turbine simulator based on speed and torque of a dc motor to drive actually loaded generators," in *Proc. 1995 First IEEE Int. Caracas Conf. Devices, Circuits Syst.*, 1995, pp. 89–93.

[11] P. E. Battaiotto, R. J. Mantz, and P. F. Puleston, "A wind turbine emulator based on a dual DSP processor system," *Contr. Eng. Pract.*, vol. 4, pp. 1261–1266, 1996.

[12] D. Parker, "Computer based real-time simulator for renewable energy converters," in *Proc. First IEEE International Workshop on Electronic Design, Test and Applications*, Jan. 2002, pp. 280–284.

[13] Y. Matsumoto, H. Umida, and S. Ozaki, "Dynamic simulator of the mechanical system," in *Proc. IECON*, Oct. 1991, vol. 1, pp. 527–532.

[14] J. B. Ekanayake, L. Holdsworth, W. XueGuang, and N. Jenkins, "Dynamic modeling of doubly fed induction generator wind turbines," *IEEE Trans. Power Syst.*, vol. 18, no. 2, pp. 803–809, May 2003.

[15] D. J. Trudnowski, A. Gentile, J. M. Khan, and E. M. Petritz, "Fixed-speed wind-generator and wind-park modeling for transient stability studies," *IEEE Trans. Power Syst.*, vol. 19, no. 4, pp. 1911–1917, Nov. 2003.

[16] J. Cidras and A. E. Feijoo, "A linear dynamic model for asynchronous wind turbines with mechanical fluctuations," *IEEE Trans. Power Syst.*, vol. 17, no. 3, pp. 681–687, Aug. 2002.

[17] P. Sorensen, A. D. Hansen, and P. A. C. Rosas, "Wind models for simulation of power fluctuations from wind farms," *J. Wind Eng. Ind. Aerodynam.*, vol. 90, pp. 1381–1402, Dec. 2002.

[18] D. A. Spera, *Wind Turbine Technology*. New York: ASME Press, 1994.

[19] R. W. Thresher, A. D. Wright, and E. L. Hershberg, "A computer analysis of wind turbine blade dynamic loads," *ASME J. Solar Energy Eng.*, vol. 108, pp. 17–25, 1986.

[20] E. N. Hinrichsen and P. J. Nolan, "Dynamics and stability of wind turbine generators," *IEEE Trans. Power App. Syst.*, vol. 101, pp. 2640–2648, Aug. 1982.

[21] O. Garcia. (1998). *Wind Turbine Dynamic Modelling*, [Online]. Available: www.iit.upco.es/oscar/download/model.ps

Dale S. L. Dolan (S'05) received the B.Sc. (Honors) degree in biology and B.Ed. degree from the University of Western Ontario, London, ON, Canada, in 1995 and 1997, respectively. He received the BASc. and MASc. degrees from the Department of Electrical and Computer Engineering, University of Toronto, Toronto, in 2003 and 2005, respectively, both in electrical engineering. He is currently working toward the Ph.D. degree at the Department of Electrical and Computer Engineering, University of Toronto.

His research interests include wind turbine emulation, alternative energy conversion systems, power electronics, and electromagnetics.

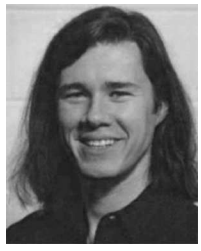

Peter W. Lehn (S'95–M'99–SM'05) received the B.Sc. and M.Sc. degrees from the University of Manitoba, Winnipeg, MB, Canada, in 1990 and 1992, respectively, both in electrical engineering. He received the Ph.D. degree in electrical engineering from the University of Toronto, Toronto, ON, in 1999.

From 1992 to 1994, he was with the Network Planning Group of Siemens AG, Erlangen, Germany. Currently, he is working as an Associate Professor at the University of Toronto.